Inorg. Chem. **2008**, *47*, 8473−8486

Forum

Structures, Physical Properties, and Chemistry of Layered Oxychalcogenides and Oxypnictides

Simon J. Clarke,* Paul Adamson, Sebastian J. C. Herkelrath, Oliver J. Rutt, Dinah R. Parker, Michael J. Pitcher, and Catherine F. Smura

Inorganic Chemistry Laboratory, Department of Chemistry, University of Oxford, South Parks Road, Oxford OX1 3QR, U.K.

Received May 31, 2008

A series of layered oxychalcogenide and oxypnictide solids is described that contain oxide layers separated by distinct layers, which contain the softer chalcogenide (S, Se, Te) or pnictide (P, As, Sb, Bi) anions. The relationships between the crystal structures adopted by these compounds are described, and the physical and chemical properties of these materials are related to the structures and the properties of the elements. The properties exhibited by the oxychalcogenide materials include semiconductor properties, for example, in LaOCuCh (Ch = chalcogenide) and derivatives, unusual magnetic properties exhibited by the class $Sr_2MO_2Cu_{2-\delta}S_2$ (M = Mn, Co, Ni), and redox properties exhibited by the materials $Sr_2MnO_2Cu_{2m-0.5}S_{m+1}$ (m = 1−3) and $Sr_4Mn_3O_{7.5}Cu_2Ch_2$ (Ch = S, Se). Recent results in the oxychalcogenide area are reviewed, and some new results on the intriguing series of compounds $Sr_2MO_2Cu_{2-\delta}S_2$ (M = Mn, Co, Ni) are reported. Oxypnictides have received less recent attention, but this is changing: a new frenzy of research is underway following the discovery of high-temperature superconductivity (>40 K) in derivatives of the layered oxyarsenide LaOFeAs. The early results in this exciting new area will be reviewed.

1. Introduction

1.1. Mixed-Anion Compounds. Oxides are ubiquitous on Earth, and the crust and mantle are composed very largely of oxides. All of the chemical elements apart from the lighter noble gases form compounds with oxygen, and so the exploration of the structures and properties of synthetic oxides dominates much of solid-state and materials chemistry and solid-state physics. Many of the Articles constituting this *Inorganic Chemistry* Forum are concerned with the synthesis, chemistry, and physics of certain oxides. Oxides as a class exhibit such a wide range of physical and chemical properties that they find uses in such diverse areas as heterogeneous catalysis, magnetic materials, electronic materials, and energy materials. Some classes of oxides are extremely famous: today rechargeable lithium cobaltate batteries[1] are widely used in mobile electronic devices, and 20 years ago the discovery of high-temperature superconductivity in certain layered cuprates[2] started a frenzy of research in solid-state chemistry and physics; yet, to underline the complexity of strongly correlated electron systems, there is as yet no reliable and predictive theory that explains why these compounds superconduct. While the synthesis of new oxides may not be simple, it may generally be carried out in air or an oxygen-rich atmosphere. As techniques for handling air-sensitive materials have become more widely available, exploration of other classes of solids containing other anions has become more routine and metal nitrides such as GaN have recently become important technological materials.[3] In oxide chemistry, it is common to make ternary or higher compounds in which different metal ions with different sizes and chemical requirements are incorporated, and much of solid-state chemistry is concerned with controlling the electron count, bond lengths and angles, and hence material properties via

* To whom correspondence should be addressed. E-mail: simon.clarke@chem.ox.ac.uk. Tel: +44 1865 272600. Fax: +44 1865 272690.

(1) Mizushima, K.; Jones, P. C.; Wiseman, P. J.; Goodenough, J. B. *Mater. Res. Bull.* **1980**, *15*, 783.

(2) Bednorz, J. G.; Muller, K. A. *Z. Phys. B: Condens. Matter* **1986**, *64*, 189.

(3) Nakamura, S.; Mukai, T.; Senoh, M. *Appl. Phys. Lett.* **1994**, *64*, 1687.

10.1021/ic8009964 CCC: $40.75 © 2008 American Chemical Society
Published on Web 09/29/2008

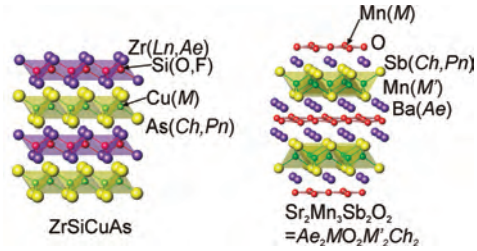

Figure 1. Structures of ZrSiCuAs[5] (left) and $Sr_2Mn_3Sb_2O_2$[6] (right), which are the basic intergrowth structure types for a large range of layered oxychalcogenides and oxypnictides. The range of species that can occupy the various crystallographic sites (ignoring dopants) is indicated. Ln = lanthanide; Ae = alkaline earth; M, M′ = transition or main group metals; Ch = chalcogenide; Pn = pnictide. Several related structures are depicted along with these two in Figure 2. In the $Sr_2Mn_3Sb_2O_2$ structure type, one Mn ion is in square-planar coordination by oxide and longer bonds to Sb complete a distorted octahedral environment. A second Mn ion is in tetrahedral coordination by Sb, so a convenient formulation is $Sr_2MnO_2Mn_2Sb_2$.

metal ion substitutions. Little attention has been given to the control of properties using the anion dimension; in this Forum Article, recent progress in the area of mixed-anion chemistry will be described with a particular focus on the areas of oxychalcogenide and oxypnictide chemistry. Here crystalline solids are considered in which oxide anions and chalcogenide (sulfide, selenide, or telluride) or pnictide (phosphide, arsenide, antimonide, or bismuthide) ions are incorporated, along with one or more cations formed from the metallic elements. The Forum Article will describe the structures, properties, and chemistry of some of these materials using selected examples and will suggest potential areas for future application of these materials.

1.2. Anion Order versus Disorder. In some mixed-anion compounds such as oxide−nitrides and oxide−fluorides, the anions are similar in size and fairly similar in their chemical requirements, so they occupy very similar crystallographic sites. This often means that ordering of the anions takes place only on short length scales, and on the length scale probed by diffraction methods, the anions appear disordered. In the general cases where an anion from the first row of the periodic table (usually oxide) is present with an anion from the second row or below, long-range anion ordering may be expected solely on the basis of the size of the anions. Because anions such as sulfide are much more polarizable than oxide, ordering of the different anions is also expected on the basis of their different chemistries. A convenient way for ordering to occur is for layered crystal structures to be adopted. Because the utility and unusual physics of many compounds arise from their layered crystal structures, the examples considered in this Forum Article will comprise compounds composed of distinct oxide and chalcogenide or pnictide layers.

1.3. Structure Types and Their Interrelationships. 1.3.1. ZrSiCuAs ($HfCuSi_2$) and $Sr_2Mn_3Sb_2O_2$ Structure Types. Two structure types, highlighted in Figure 1 and shown in the structure map shown in Figure 2, dominate the known chemistry of oxychalcogenides and are also well-represented by oxide−pnictides and other compounds. These structure types have great flexibility and are each merely the most common members of the structural homologous series.

The oxysulfide LaOCuS, originally reported by Palazzi in 1981,[4] is a representative of the "filled" PbFCl structure type (Figure 1) originally reported for ZrSiCuAs,[5] (and which is referred to currently in the ICSD as the $HfCuSi_2$ structure type). The formulation as LaOCuS emphasizes the occurrence of two fairly distinct layer types, formally $[LaO]^+$ and $[CuS]^-$, and we will use this formulation throughout for this and related layered compounds. These layers are respectively of the PbO and anti-PbO types, and as will become clearer below, they are also conveniently thought of as fragments of the fluorite and antifluorite structure types, respectively. In LaOCuS, the oxide ion is tetrahedrally coordinated solely by the electropositive Ln ion and the chalcophilic monovalent Cu ion is coordinated tetrahedrally solely by sulfide.

The second important structure type is that first described for the oxide antimonide $Sr_2Mn_3Sb_2O_2$[6] (which may conveniently be formulated as $Sr_2MnO_2Mn_2Sb_2$) and related oxide pnictides[7,8] and later found for $Sr_2ZnO_2Cu_2S_2$ in some pioneering work in the oxysulfide area by Zhu and Hor in 1997.[9] In $Sr_2ZnO_2Cu_2S_2$, the chalcogenide layer $[Cu_2S_2]^{2-}$ is similar to that in LaOCuS, while the $[Sr_2ZnO_2]^{2+}$ oxide layer contains ZnO_2 planar sheets separated from the $[Cu_2S_2]^{2-}$ layer by Sr ions. Several oxychalcogenides[10,11] and oxypnictides[7,8] have been reported with this crystal structure, and the intriguing crystal chemistry and properties of some of the oxychalcogenide members containing middle-to-late first-row transition-metal ions in the oxide layers are summarized in section 2.

1.3.2. Homologues with Thicker Chalcogenide or Oxide Layers. We have recently reported oxychalcogenides with structures related to the $Sr_2ZnO_2Cu_2S_2$ ($Sr_2Mn_3Sb_2O_2$) structure type in which thicker copper sulfide layers are stabilized in the series $Sr_2MnO_2Cu_{2m-\delta}S_{m+1}$ ($m = 1-3$; $\delta \sim 0.5$), which all have very similar Sr_2MnO_2 layers.[12−15] These $Cu_{2m-\delta}S_{m+1}$ fragments are clearly recognizable fragments of the antifluorite structure of α-Cu_2S. Other workers have reported on structural relatives in which the familiar $[Cu_2S_2]^{2-}$ layers are separated by oxide layers of variable thickness, which are recognizable fragments of the perovskite structure. Thus, $Sr_3M_2O_5Cu_2S_2$ (M = Fe,[16] Sc[11]) and $A_4Mn_3O_{8-\delta}Cu_2Ch_2$ (A = Sr, Ba; Ch = S, Se; $\delta \sim 0.5$)[17−19] are respectively the *n*

(4) Palazzi, M. *C. R. Seances Acad. Sci., Ser. C* **1981**, *292*, 7899.
(5) Johnson, V.; Jeitschko, W. *J. Solid State Chem.* **1974**, *11*, 161.
(6) Brechtel, E.; Cordier, G.; Schaefer, H. *Z. Naturforsch., B: Anorg. Chem., Org. Chem.* **1979**, *34*, 777.
(7) Enjalran, M.; Scalettar, R. T.; Kauzlarich, S. M. *Phys. Rev. B* **2000**, *61*, 14570.
(8) Ozawa, T. C.; Kauzlarich, S. M.; Bieringer, M.; Wiebe, C. R.; Greedan, J. E.; Gardner, J. S. *Chem. Mater.* **2001**, *13*, 973.
(9) Zhu, W. J.; Hor, P. H. *J. Solid State Chem.* **1997**, *130*, 319.
(10) Zhu, W. J.; Hor, P. H.; Jacobson, A. J.; Crisci, G.; Albright, T. A.; Wang, S.-H.; Vogt, T. *J. Am. Chem. Soc.* **1997**, *119*, 12398.
(11) Otzschi, K.; Ogino, H.; Shimoyama, J.; Kishio, K. *J. Low Temp. Phys.* **1999**, *117*, 729.
(12) Gál, Z. A.; Rutt, O. J.; Smura, C. F.; Overton, T. P.; Barrier, N.; Clarke, S. J.; Hadermann, J. *J. Am. Chem. Soc.* **2006**, *128*, 8530.
(13) Barrier, N.; Clarke, S. J. *Chem. Commun.* **2003**, 164.
(14) Rutt, O. J.; Williams, G. R.; Clarke, S. J. *Chem. Commun.* **2006**, 2869.
(15) Indris, S.; Cabana, J.; Rutt, O. J.; Clarke, S. J.; Grey, C. P. *J. Am. Chem. Soc.* **2006**, *128*, 13354.
(16) Zhu, W. J.; Hor, P. H. *J. Solid State Chem.* **1997**, *134*, 128.
(17) Zhu, W. J.; Hor, P. H. *J. Solid State Chem.* **2000**, *153*, 26.

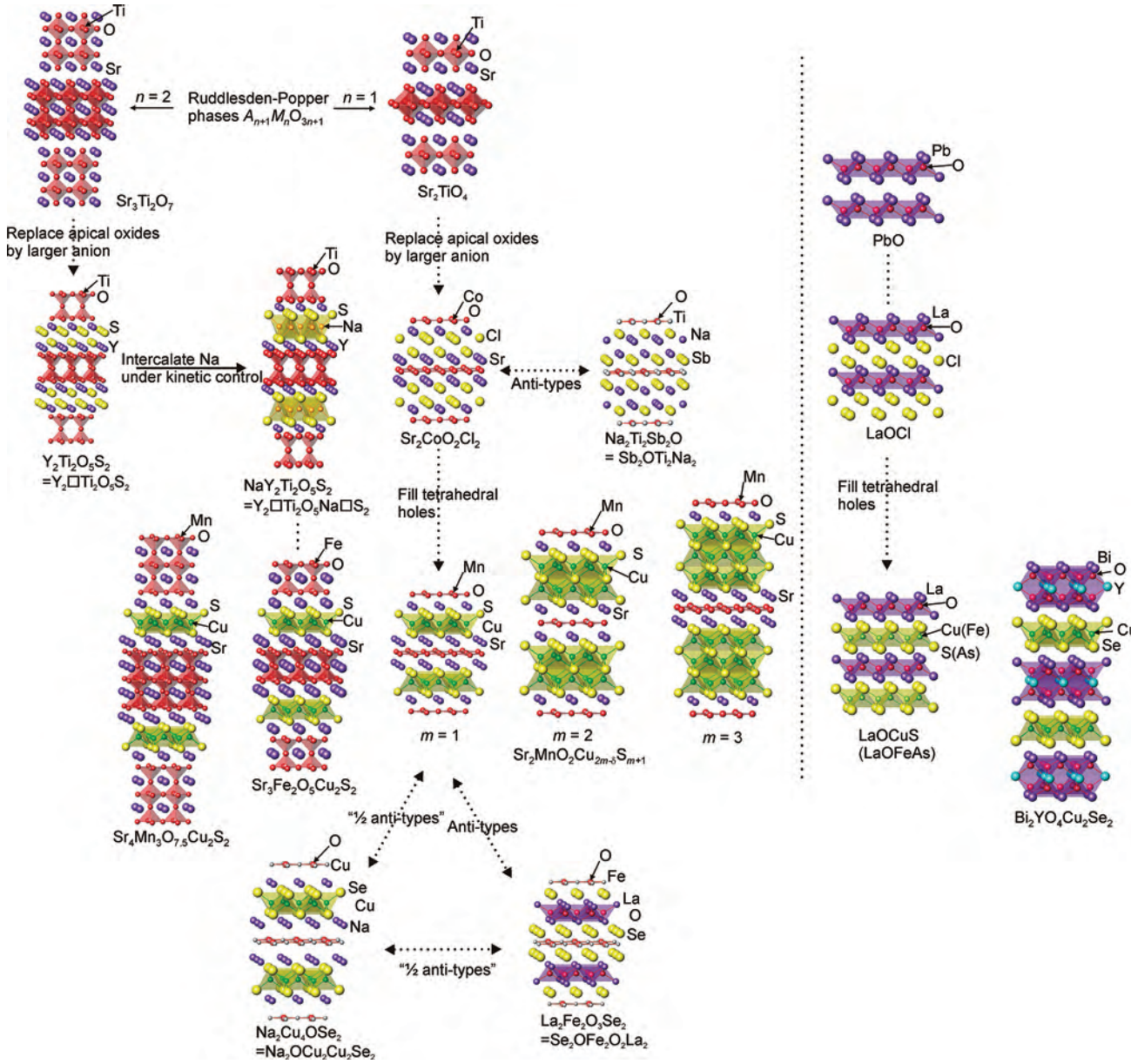

Figure 2. Relationships between the crystal structures of layered oxychalcogenides and oxypnictides described in this Forum Article. The diagram shows the formal relationship between the Ruddlesden−Popper structures well-known in oxide chemistry and oxychalcogenide and oxyhalide derivatives, which may be obtained by substituting the oxide ions in the rock-salt-type layers by the larger anions. The structures of many oxychalcogenides and oxypnictides are then formally (and in one case actually) derived from these structures by the insertion of cations into tetrahedral holes in the layers formed by the large anions; i.e., the structure of $Sr_2MO_2Cu_2Ch_2$ is derived from that of $Sr_2MO_2Cl_2$ (M = first-row transition metal) in the same way that the structure of LaOCuCh is derived from that of LaOCl. Several members of homologous series $A_{n+1}M_nO_{3n-1}Cu_{2m}S_{m+1}$ (A = alkaline earth; M = transition metal) are known, and some antitype relationships between structures are known. The structural relationships are described further in the text.

= 2 and 3 members of the homologous series $A_{n+1}M_nO_{3n-1}Cu_2S_2$, which is most well represented by the $n = 1$ members. Some analogues, $Sr_3Fe_2O_5Ag_2Ch_2$,[20] are known, with Ag^+ ions replacing Cu^+ ions in the chalcogenide layer. Other structural relatives of the $A_{n+1}M_nO_{3n-1}Cu_2S_2$ compounds with different oxide layer structures are known.[17,21] Evans and co-workers described the compounds $Bi_2LnO_4Cu_2Se_2$ (Ln = Y, Gd, Sm, Nd, La), which are related to the ZrSiCuAs structure of LaOCuS by an increase in the thickness of the oxide layer so that it resembles a fragment of the fluorite structure.[22] $CeOBiS_2$[23] contains a fluorite-type Ce_2O_2 layer, which intergrows with a rock-salt-type Bi_2S_4 layer; the structures of this and other layered oxychalcogenides have been described elsewhere,[24] and the discussion of these and other layered oxypnictides[25] lies outside the immediate scope of this Forum Article.

1.3.3. Formal Relationships between Structures. Figure 2 shows some of the formal relationships that exist between the important structures exhibited by oxychalcogenides and oxypnictides and other crystal structures that are widely represented in solid-state chemistry.

(18) Hyett, G.D. Phil. Thesis, University of Oxford, Oxford, U.K., 2006.
(19) Hyett, G.; Barrier, N.; Clarke, S. J.; Hadermann, J. *J. Am. Chem. Soc.* **2007**, *129*, 11192.
(20) Cario, L.; Lafond, A.; Morvan, T.; Kabbour, H.; André, G.; Palvadeau, P. *Solid State Sci.* **2005**, *7*, 936.

The Ruddlesden−Popper[26] oxides $A_{n+1}M_nO_{3n+1}$ ($n = 1-4$) are an important class of solid-state compounds, and the $n = \infty$ member is the cubic perovskite AMO_3. A limited number of sulfides, e.g., $Ba_{n+1}Zr_nS_{3n+1}$ ($n = 1$,[27,28] 2,[28,29] 3[30]), are also known with these structures. The oxides may be described in the following way: MO_6 octahedra share their equatorial vertexes to form a sheet, and n such sheets are stacked via sharing of the remaining vertexes to form a perovskite-type block in which A cations are normally incorporated into 12-coordinate voids by oxide anions. These perovskite-type blocks are separated by 9-coordinate A cations, which together with the unshared apical anions of the perovskite blocks form so-called rock-salt layers. Several compounds are closely related to the Ruddlesden−Popper oxides by the replacement of the unshared apical anions of the perovskite blocks (i.e., the anions in the rock-salt layers) by larger anions such as halide or sulfide. The structures of the oxyhalides $A_{n+1}M_nO_{3n-1}Hal_2$, such as $Sr_2CuO_2Cl_2$[31] and $Sr_2CoO_2Cl_2$[32] depicted in Figure 2, are formally derived from the structures of the Ruddlesden−Popper compounds in this way.

The structures of the series $Ln_2\square Ti_2O_5S_2$[33,34] are similarly formally related to the $n = 2$ Ruddlesden−Popper type structure of $Sr_3Ti_2O_7$ by replacement of the oxide ions in the rock-salt layers by sulfide. In this particular case, a vacancy is also incorporated: the 12-coordinate cation site in the center of the perovskite block. These titanate oxysulfides have generated some interest as possible candidate materials for the photocatalytic splitting of water.[35] We have shown that these titanates may be reduced by intercalation of alkali metals, and under the appropriate reaction conditions, sodium[36,37] and lithium[38] may occupy sites in the center of the oxide layer. The lithiated derivatives, in particular, show interesting electronic and structural properties as a function of the lithium content including an insulator-to-metal transition with an associated phase gap region around $Li_{0.6}Y_2Ti_2O_5S_2$ and an electronically driven structural distortion.[38] Furthermore, we have shown[36,39] that insertion of sodium at low temperatures proceeds such that Na^+ ions are incorporated into the rock-salt-type sulfide layers in β-$NaLn_2Ti_2O_5S_2$ and occupy half the tetrahedral sites, which are occupied by Cu^+ ions in the structure of $Sr_3Fe_2O_5Cu_2S_2$. We can write the formula of β-$NaLn_2Ti_2O_5S_2$ as $Ln_2\square Ti_2O_5Na\square S_2$ to emphasize the structural relationship with $Sr_3Fe_2O_5Cu_2S_2$, which is also shown in Figure 2. To summarize, formally the chalcogenide ions in $A_{n+1}M_nO_{3n-1}Cu_2S_2$ take the place of the oxide ions in the "rock-salt"-type layers of the Ruddlesden−Popper compounds, and the oxychalcogenides contain additional ions (usually Cu^+) that occupy tetrahedral sites in the resulting chalcogenide layers.

This formal relationship between certain oxychalcogenides and the Ruddlesden−Popper structures is mirrored in the formal relationship between the structure of PbFCl or LnOCl and that of LaOCuS; i.e., the structure of LaOCuS is derived from that of LaOCl by replacement of chloride by sulfide and the incorporation of the Cu^+ ions into tetrahedral sites coordinated by sulfide ions. Thus, the ZrSiCuAs (or $HfCuSi_2$) structure of LaOCuS is also often described as the "stuffed" or "filled" PbFCl structure.[5] The prediction and realization of the "filled" PbFCl structure and several other useful structural interrelationships are discussed in the original report on ZrCuSiAs.[5] Compounds with the ZrSiCuAs structure type have recently been reviewed.[40]

1.3.4. Antitype Structures. The structure adopted by $Sr_2MnO_2Mn_2Sb_2$,[6] $Sr_2ZnO_2Cu_2S_2$,[9] and others is also known in forms that might be described as the "half-antitype" and "full-antitype" in terms of the occupation of the various crystallographic sites by anions or cations. The compound $La_2Fe_2O_3Se_2$ originally reported by Mayer and co-workers[41] consists of La_2O_2 PbO-type (fluorite-type) layers similar to those in LaOCuS and Fe_2O sheets in which O is in square-planar coordination by Fe. These two cationic oxide-containing layers are separated by selenide ions. Fe is thus coordinated linearly by O and also by four selenide ions, which complete a distorted FeO_2Se_4 octahedron. The compound might be formulated as $Se_2OFe_2O_2La_2$ to emphasize the antitype relationship with $Sr_2ZnO_2Cu_2S_2$ in terms of the anion and cation distribution. An intriguing compound with a similar structure, which is formally the "half-antitype" of both these, is $Na_{1.9}Cu_4OSe_3$ reported by Kanatzidis and co-workers[42] in which Cu_2Se_2 anti-PbO (antifluorite) layers are separated from Cu_2O square planes by Na ions. This might be formulated as $Na_{1.9}OCu_2Cu_2Se_2$ for comparison with the other compounds. It was found to be slightly Na-deficient (the ideal formula would be $Na_2Cu_4OSe_3$), and band structure

(21) Hyett, G.; Gál, Z. A.; Smura, C. F.; Clarke, S. J. *Chem. Mater.* **2008**, *20*, 559.
(22) Evans, J. S. O.; Brogden, E. B.; Thompson, A. L.; Cordiner, R. L. *Chem. Commun.* **2002**, 912.
(23) Ceolin, R.; Rodier, N. *Acta Crystallogr., Sect. B* **1976**, *32*, 1476.
(24) Guittard, M.; Benazeth, S.; Dugue, J.; Jaulmes, S.; Palazzi, M.; Laruelle, P.; Flahaut, J. *J. Solid State Chem.* **1984**, *51*, 227.
(25) Cava, R. J.; Zandbergen, H. W.; Krajewski, J. J.; Siegrist, T.; Hwang, H. Y.; Batlogg, B. *J. Solid State Chem.* **1997**, *129*, 250.
(26) Ruddlesden, S. N.; Popper, P. *Acta Crystallogr.* **1958**, *11*, 54.
(27) Chen, B.-H.; Eichhorn, B. W. *Mater. Res. Bull.* **1991**, *26*, 1035.
(28) Saeki, M.; Yajima, Y.; Onoda, M. *J. Solid State Chem.* **1991**, *92*, 286.
(29) Chen, B.-H.; Eichhorn, B. W.; Wong-Ng, W. *Acta Crystallogr., Sect. C* **1994**, *50*, 161.
(30) Chen, B.-H.; Wong-Ng, W.; Eichhorn, B. W. *J. Solid State Chem.* **1993**, *103*, 75.
(31) Grande, B.; Müller-Buschbaum, H. *Z. Anorg. Allg. Chem.* **1976**, *417*, 68.
(32) Knee, C. S.; Weller, M. T. *J. Solid State Chem.* **2002**, *168*, 1.
(33) Boyer, C.; Deudon, C.; Meerschaut, A. *C. R. Acad. Sci. Paris, Ser. II* **1999**, *2*, 93.
(34) Goga, M.; Seshadri, R.; Ksenofontov, V.; Gütlich, P.; Tremel, W. *Chem. Commun.* **1999**, 979.
(35) Ishikawa, A.; Takata, T.; Kondo, J. N.; Hara, M.; Kobayashi, H.; Domen, K. *J. Am. Chem. Soc.* **2002**, *124*, 13547.
(36) Denis, S. G.; Clarke, S. J. *Chem. Commun.* **2001**, 2356.
(37) Clarke, S. J.; Denis, S. G.; Rutt, O. J.; Hill, T. L.; Hayward, M. A.; Hyett, G.; Gál, Z. A. *Chem. Mater.* **2003**, *15*, 5065.
(38) Hyett, G.; Rutt, O. J.; Gál, Z. A.; Denis, S. G.; Hayward, M. A.; Clarke, S. J. *J. Am. Chem. Soc.* **2004**, *126*, 1980.
(39) Rutt, O. J.; Hill, T. L.; Gál, Z. A.; Hayward, M. A.; Clarke, S. J. *Inorg. Chem.* **2003**, *42*, 7906.
(40) Pöttgen, R.; Johrendt, D. *Z. Naturforsch., B: Chem. Sci.* **2008**, submitted for publication.
(41) Mayer, J. M.; Schneemeyer, L. F.; Siegrist, T.; Waszczak, J. V.; Van Dover, B. *Angew. Chem., Int. Ed. Engl.* **1992**, *31*, 1645.
(42) Park, Y.; DeGroot, D. C.; Schindler, J. L.; Kannewurf, C. R.; Kanatzidis, M. G. *Chem. Mater.* **1993**, *5*, 8.

calculations[43] showed that the holes introduced by this slight deficiency should reside in bands derived from the Cu_2Se_2 layers, which may readily be depleted as described below. In contrast to the situation in the compounds $Sr_2ZnO_2Cu_2Ch_2$ and $Ch_2OFe_2O_2La_2$ (Ch = S, Se), in $Na_2OCu_2Cu_2Se_2$ the ions that lie closest to the Na^+ cation are the Se^{2-} ions in the Cu_2Se_2 layer and the Cu^+ ions in the Cu_2O layers, with the result that Cu^+-Na^+ repulsion increases the interplanar separation relative to that in $Sr_2ZnO_2Cu_2Ch_2$ or $Ch_2OFe_2O_2La_2$ (Ch = S, Se). The compounds all crystallize in the space group *I*4/*mmm*, and in $Sr_2ZnO_2Cu_2Ch_2$ and $Ch_2OFe_2O_2La_2$, the *c*/*a* ratios are all between 4.42 and 4.57 for the four compounds with Ch = S, Se. In $Na_2OCu_2Cu_2Se_2$, the *c*/*a* ratio is 22% larger (5.52), so the compound is much more anisotropic. An antitype relationship also exists between the oxyhalides $Sr_2CuO_2Cl_2$[31] and $Sr_2CoO_2Cl_2$[32] depicted in Figure 2 and the oxypnictides $Na_2Ti_2Pn_2O$ (=$Pn_2OTi_2Na_2$; Pn = As, Sb).[44−46]

The common feature of the structures described above and that are of interest in this Forum Article is that while the compounds may contain five elements in distinct chemical environments, there are relatively few structural variables. In the remainder of the Forum Article, we will survey the synthesis, important structural details, physical properties, and chemistry of compounds with the main structure types described above, with a slight bias toward compounds that are the subject of work that is in progress in our group.

1.4. General Electronic Considerations. The compounds LaOCuS and $Sr_2ZnO_2Cu_2S_2$, which represent the two main structure types described above, are band-gap insulators. Photoelectron spectroscopy measurements and band structure calculations on such compounds[47] clearly show that the Cu 3d levels and the S 3p levels are of very similar energies and that these form the highest occupied valence-band states. The states at the top of the valence band are antibonding states and may readily be depleted, resulting in holes that are highly mobile.[48] The compounds KCu_4S_3[49] and $TlCu_2S_2$[50] contain copper sulfide antifluorite-type layers similar to those exhibited in the oxysulfides, and these ternary sulfides are metallic with one hole per formula unit in the valence band. Similarly, $Bi_2LnO_4Cu_2Se_2$ has one hole per formula unit in the valence band.[22] Doping in the oxysulfides will be discussed below.

In compounds with structures similar to those of $Sr_2ZnO_2Cu_2S_2$ and those that feature thicker oxide layers, middle-to-late transition-metal ions may readily be accommodated in the oxide layers in place of Zn. In such cases, the transition-metal 3d states are localized states that lie above the Cu 3d/S 3p band, and such compounds display a range of magnetic properties resulting from the interactions of magnetic moments localized on the transition-metal ions. In such cases, the transition-metal ions are in unusual coordination environments. For example, in $A_2MnO_2Cu_{2-\delta}S_2$ and $A_2CoO_2Cu_2S_2$ (A = Sr, Ba), the transition-metal ions are in extremely square-planar environments. These are not commonly encountered in oxides of the first-row transition metals synthesized in conventional high-temperature solid-state reactions, although recently low-temperature topotactic reduction of perovskites has yielded NiO_2 square-planar layers in $LaNiO_2$ (Ni^+)[51,52] and FeO_2 square-planar layers in $Sr_{1-x}Ca_xFeO_2$.[53,54] The antitype compound $La_2Fe_2O_3Se_2$ (=$Se_2OFe_2O_2La_2$)[41] with an unusual distorted octahedral FeO_2Se_4 coordination environment for Fe^{2+} has recently been characterized as a low-dimensional magnetic material.[55]

1.5. Interplay of Oxide and Sulfide Layers and Structural Tuning. The oxide and chalcogenide or pnictide layers in these layered compounds may be considered quite electronically distinct. The degree to which this is true depends on, for example, the size of the electropositive cation A^{2+} in the $A_2MO_2Cu_2S_2$ structure, which dictates the M−S distance and hence the extent to which the transition metal M is engaged in bonding interactions with the chalcogenide anion. One other clear element of flexibility in these structures concerns the variable occupancy of the metal ion (normally Cu^+ or Ag^+) in the tetrahedral sites in the chalcogenide layer. It has already been reported that $Sr_2CoO_2Cu_2S_2$ supports a small and variable copper deficiency.[10] We have since shown that the members of the series $Sr_2MnO_2Cu_{2m-\delta}S_{m+1}$ ($m = 1-3$) all have a very substantial copper deficiency ($\delta \sim 0.5$),[12] and a range of copper deficiencies have been reported for $CeOCu_{1-\delta}S$ ($0 < \delta < 0.25$).[56,57] The implication of copper deficiency is that the transition metal or lanthanide is oxidized, and we have shown[12] using Mn K-edge XANES measurements and magnetometry backed up by bond-valence calculations that the Mn oxidation state in $Sr_2MnO_2Cu_{2m-\delta}S_{m+1}$ ($m = 1-3$; $\delta \sim 0.5$) is 2.5+, which has important implications for the magnetic properties as described in section 2.2.2. CeOCuS is the only compound in the series LnOCuS in which a copper deficiency has been confirmed,[57] consistent with Ce^{3+} being the only trivalent Ln ion that may readily be oxidized.

(43) Chacon, G.; Long, X.; Zheng, C. *J. Alloys Compd.* **1994**, *216*, 177.
(44) Adam, A.; Schuster, H. U. *Z. Anorg. Allg. Chem.* **1990**, *584*, 150.
(45) Ozawa, T. C.; Pantoja, R.; Axtell, E. A.; Kauzlarich, S. M.; Greedan, J. E.; Bieringer, M.; Richardson, J. W. *J. Solid State Chem.* **2000**, *153*, 275.
(46) Axtell, E. A.; Ozawa, T.; Kauzlarich, S. M.; Singh, R. R. P. *J. Solid State Chem.* **1997**, *134*, 423.
(47) Inoue, S.; Ueda, K.; Hosono, H.; Hamada, N. *Phys. Rev. B* **2001**, *64*, 245211.
(48) Vajenine, G. V.; Hoffmann, R. *Inorg. Chem.* **1996**, *35*, 451.
(49) Brown, D. R.; Zubieta, J. A.; Vella, P. A.; Wrobleski, J. T.; Watt, T.; Hatfield, W. E.; Day, P. *Inorg. Chem.* **1980**, *19*, 1945.
(50) Berger, R. *J. Less Common Met.* **1989**, *147*, 141.
(51) Levitz, P.; Crespin, M.; Gatineau, L. *J. Chem. Soc., Faraday Trans. 2* **1983**, *79*, 1195.
(52) Hayward, M. A.; Green, M. A.; Rosseinsky, M. J.; Sloan, J. *J. Am. Chem. Soc.* **1999**, *121*, 8843.
(53) Tsujimoto, Y.; Tassel, C.; Hayashi, N.; Watanabe, T.; Kageyama, H.; Yoshimura, K.; Takano, M.; Ceretti, M.; Ritter, C.; Paulus, W. *Nature* **2007**, *450*, 1062.
(54) Tassel, C.; Watanabe, T.; Tsujimoto, Y.; Hayashi, N.; Kitada, A.; Sumida, Y.; Yamamoto, T.; Kageyama, H.; Takano, M.; Yoshimura, K. *J. Am. Chem. Soc.* **2008**, *130*, 3764.
(55) Kabbour, H.; Janod, E.; Corraze, B.; Danot, M.; Lee, C.; Whangbo, M.-H.; Cario, L. *J. Am. Chem. Soc.* **2008**, *130*, 8261.
(56) Charkin, D. O.; Akopyan, A. V.; Dolgikh, V. A. *Russ. J. Inorg. Chem. (Transl. Zh. Neorg. Khim.)* **1999**, *44*, 833.
(57) Chan, G. H.; Deng, B.; Bertoni, M.; Ireland, J. R.; Hersam, M. C.; Mason, T. O.; Van Duyne, R. P.; Ibers, J. A. *Inorg. Chem.* **2006**, *45*, 8264.

2. Compounds and Their Properties

The following sections give brief descriptions of potentially important and chemically interesting compounds in the classes of layered oxychalcogenides and oxypnictides. In all these cases, the compounds that will be described are the subject of current research, some of it very intense. Section 2.1 discusses examples that may be characterized as band-gap insulators and discusses the structural tuning and electronic doping that is possible in these compounds and that is relevant in the field of transparent conductors. Section 2.2 discusses some selected examples describing the diverse electronic and magnetic properties of layered oxychalcogenides and oxypnictides; included here is the recent discovery, 20 years after the discovery of the layered cuprate superconductors, of a new class of high-temperature superconductors based on transition-metal pnictide layers. Section 2.3 describes the chemical properties of certain layered oxychalcogenides including potential applications as Li ion secondary battery electrode materials. The examples have been chosen so as to illustrate many of the exotic structural and electronic features of these materials.

2.1. Structures, Property Tuning, and Doping in Band-Gap Insulators. 2.1.1. LnCuOCh and Isostructural Derivatives. The layered oxychalcogenides that have received the greatest attention are LnOCuCh (Ln = lanthanide, Ch = S, Se, Te). These compounds have been extensively studied through property measurements, structural analysis, and computational approaches largely because the compounds show promise as transparent p-type conductors. The work in this area has been reviewed recently by Ueda and Hosono and co-workers,[58−60] and we will only briefly survey the work that has been reported on these and isostructural fluoride−chalcogenide materials. In these compounds, there is evidence from the optical properties, large band gaps, and large exciton binding energies that because of the highly anisotropic nature of the crystal structures the compounds can, in some respects, be considered as "quantum-well-like" materials in which there is a charge-carrying chalcogenide layer separated by an insulating oxide layer.[58,59]

These oxychalcogenides are wide-band-gap semiconductors with band gaps of around 3 eV for the oxysulfides. Chemical intuition supported by band-structure calculations[48] suggests that the states at the top of the valence band are composed of antibonding Cu 3d/Ch *n*p states and antibonding Cu 3d/Cu 3d states while the states at the bottom of the conduction band are mainly Cu 4s/Ln 5d/Ch *n*p antibonding states. The band gap in these materials is tuned by changing the chalcogenide or by changing the dispersion of the valence and conduction bands by changing the lattice parameters via selection of the Ln ion.

The band gaps in LnOCuCh are correlated with the electronegativity of the chalcogenide: LaOCuS with a band gap of 3.1 eV and LaOCuSe (2.82 eV) are wide-band-gap insulators, while LaOCuTe with a significantly narrower gap (2.31 eV) behaves as a degenerate semiconductor.[61] For a given chalcogenide ion, decreasing the size of the Ln ion results in a decrease of the band gap. The LnCuOSe systems support trivalent cations as small as Y^{3+} (and Ho^{3+}), but not smaller,[62] and the band gap in YOCuSe of 2.58 eV is significantly smaller than that in LaOCuSe (2.82 eV).[63] This is principally ascribed to the shortening of the basal lattice parameter, and hence the Cu−Cu distance in the Cu_2Se_2 layers, resulting in broadening of the valence and conduction bands. The correlation of the band gap with the identity of the chalcogenide and the basal lattice parameter for several LnOCuCh phases as well as isostructural fluoride chalcogenides and other structural relatives is shown in Figure 3. Substitution of the Ln ions by trivalent Bi ions is possible[64] and results in a very significant decrease in the band gap to below 1.5 eV in BiOCuS principally due to the lowering of the energy of the Bi 6p orbitals forming the conduction band minimum due to relativistic effects.[65] All these compounds are generally synthesized using conventional solid state techniques under anaerobic conditions. A convenient hydrothermal synthesis of BiOCuS has recently been reported.[65]

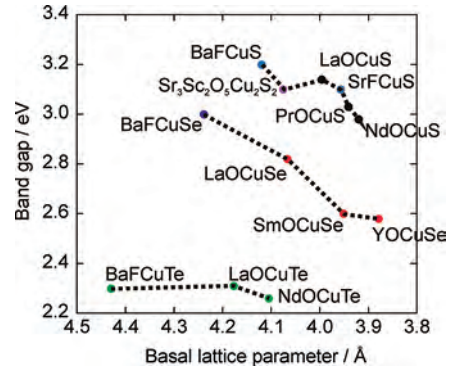

Figure 3. Correlation between the band gap, basal lattice parameter, and composition for a series of layered oxychalcogenides and fluoride chalcogenides, which are of interest in the context of transparent conducting materials.

Isostructural materials include the fluoride chalcogenides AFCuCh (A = Sr,[66] Ba,[67] Eu[68]) in which fluorite-type A_2F_2 cationic layers are separated by Cu_2Ch_2 anionic layers similar to those in the oxychalcogenides. The band gaps of these compounds follow the trend with the lattice parameter shown

(58) Ueda, K.; Hiramatsu, H.; Hirano, M.; Kamiya, T.; Hosono, H. *Thin Solid Films* **2006**, *496*, 8.
(59) Hosono, H. *Thin Solid Films* **2007**, *515*, 6000.
(60) Ohta, H.; Nomura, K.; Hiramatsu, H.; Ueda, K.; Kamiya, T.; Hirano, M.; Hosono, H. *Solid-State Electron.* **2003**, *47*, 2261.
(61) Liu, M.-L.; Wu, L.-B.; Huang, F.-Q.; Chen, L.-D.; Ibers, J. A. *J. Solid State Chem.* **2007**, *180*, 62.
(62) Berdonosov, P. S.; Kusainova, A. M.; Kholodkovskaya, L. N.; Dolgikh, V. A.; Akselrud, L. G.; Popovkin, B. A. *J. Solid State Chem.* **1995**, *118*, 74.
(63) Ueda, K.; Takafuji, K.; Yanagi, H.; Kamiya, T.; Hosono, H.; Hiramatsu, H.; Hirano, M.; Hamada, N. *J. Appl. Phys.* **2007**, *102*, 113714.
(64) Kusainova, A. M.; Berdonosov, P. S.; Akselrud, L. G.; Kholodkovskaya, L. N.; Dolgikh, V. A.; Popovkin, B. A. *J. Solid State Chem.* **1994**, *112*, 189.
(65) Sheets, W. C.; Stampler, E. S.; Khabbour, H.; Bertoni, M. I.; Cario, L.; Mason, T. O.; Marks, T. J.; Poeppelmeier, K. R. *Inorg. Chem.* **2007**, *46*, 10741.
(66) Khabbour, H.; Cario, L.; Jobic, S.; Corraze, B. *J. Mater. Chem.* **2006**, *16*, 4165.
(67) Zhu, W.-J.; Huang, Y. Z.; Wu, F.; Dong, C.; Chen, H.; Zhao, Z.-X. *Mater. Res. Bull.* **1994**, *29*, 505.
(68) Motomitsu, E.; Yanagi, H.; Kamiya, T.; Hirano, M.; Hosono, H. *J. Solid State Chem.* **2006**, *179*, 1668.

by the LnOCuCh members, demonstrating the similarity of the states at the top of the valence band and the bottom of the conduction band in the whole series.

The structure of LaOCuS is extremely flexible. Cario and co-workers have successfully synthesized fluoride pnictides by selecting appropriate compositions for the two types of layer. BaFZnP (band gap of approximately 2 eV), BaFMnP, BaFZnSb, and SrFZnP were all synthesized.[69] The structure is also adopted by a wide range of oxide pnictides including the LnOFeAs-derived high-temperature superconductors, which will be considered in section 2.2.3.

Because the states at the top of the valence band in LnOCuCh are antibonding states, these compounds can be doped p-type in order to produce transparent p-type conductors. In LaOCuS, holes may be introduced into the valence band by substitution of 3% of the La^{3+} ions by Sr^{2+}, and this leads to a degenerate semiconductor with an electrical conductivity roughly 5 orders of magnitude larger than that of the undoped material at room temperature and approximately temperature-independent.[70] Further doping is reported to result in metallic behavior.[71] However, these materials have rather low carrier mobility (e.g., 10 $cm^2\ V^{-1}\ s^{-1}$ for bulk LaOCuS[61] and lower values for thin-film materials), which may restrict their technological application.[61,72,73] The mobility increases as the electronegativity of the chalcogen decreases (e.g., 80 $cm^2\ V^{-1}\ s^{-1}$ for bulk LaOCuTe[61]), but this also decreases the band gap considerably. In BaFCuS and BaFCuSe, hole doping, achieved by replacing 10% of the Ba^{2+} ions by K^+ ions, results in 1000-fold enhancements of the conductivity and metallic behavior.[73] Analogously, SrFCuS may be hole-doped via aliovalent substitution on both the alkaline-earth and fluoride sites, yielding, for example, $Na_{0.1}Sr_{0.9}FCuS$ and $SrF_{0.95}O_{0.05}CuS$ with room temperature conductivities 4−5 orders of magnitude greater than those in the undoped parent and showing metallic behavior.[66] BaFCuTe has a band gap of 2.3 eV and is a degenerate p-type semiconductor.[74]

While the main focus of these studies on semiconducting LaOCuCh and their relatives has been on electronic conductivity, it should be noted that in the compounds with copper chalcogenide layers the monovalent ions are mobile like in fluorite-type Ag_2Ch and Cu_2Ch, making these compounds fast ion conductors. In the case of LaOAgS, analysis of the displacement parameters obtained from powder neutron diffraction measurements[75] clearly confirms that the Ag ion mobility is restricted to two dimensions, as would be expected for such an anisotropic crystal structure.

2.1.2. Structural Relatives of the LnOCuCh Compounds. As discussed above, the chalcogenide layers in these systems may readily accommodate vacancies in the tetrahedral sites. This is further discussed in sections 2.2.1 and 2.2.2 in the context of $CeOCu_{1-\delta}S$ and $Sr_2MnO_2Cu_{2m-\delta}S_{m+1}$, where up to one-quarter of the tetrahedral sites may be vacant. In the compounds with the ZrSiCuAs structure of the LnOCuCh series, there are two extreme possibilities for the incorporation of vacancies in the chalcogenide layer when a formally divalent ion is substituted for the Cu^+ ions in the tetrahedral sites. In $CeOMn_{0.5}Se$,[76] half of the sites are vacant in a disordered fashion, while in $La_2O_2CdSe_2$,[77] a superstructure of the LaOCuS structure is adopted in which half of the tetrahedral sites are vacant such that there are no edge-sharing $CdSe_4$ tetrahedra. $La_2O_2CdSe_2$ with a band gap of 3.3 eV has been investigated as a possible transparent conductor, but the possibilities for doping are limited compared with the compounds based on copper chalcogenide layers, and the conductivities of $La_2O_2CdSe_2$ were found to be extremely low compared with compounds containing copper chalcogenide layers.[78] This arises because in $La_2O_2CdSe_2$ the Cd 4d states lie well below the valence-band maximum, which is composed mainly of Se 4p states;[77] in contrast, the Cu 3d states are well mixed with the S 3p or Se 4p states in the valence band of the materials with copper chalcogenide layers.

2.1.3. Wide-Band-Gap Semiconductors with Perovskite-Type Oxide Layers Separating CuCh Chalcogenide Layers. Figure 2 suggests that other candidates for wide-band-gap semiconductors are those in which perovskite-type oxide layers containing d^0 or d^{10} metals separate the antifluorite-type CuCh layers. $Sr_2ZnO_2Cu_2S_2$[9] and $Sr_3Sc_2O_5Cu_2S_2$[11] and doped derivatives have been explored in the context of trying to produce viable transparent p-type conductors. $Sr_2ZnO_2Cu_2S_2$ contains ZnO_2 anionic sheets separated from Cu_2S_2 anti-PbO-type layers by Sr ions. The optical band gap is 2.7 eV, and the basal lattice parameter is 4.01 Å, which means this compound does not conform to the trend of band gap against lattice parameter shown in Figure 3. Band-structure calculations together with chemical intuition suggest that this is because the bottom of the conduction band is dominated by Zn 4s states with Cu 4s states at higher energies.[79] It has been shown that this may be doped into the metallic regime by substitution of Sr by Na in $Sr_{2-x}Na_xZnO_2Cu_2S_2$ and, with $x = 0.1$, the room temperature conductivity is 7 orders of magnitude larger than that in the undoped material.[79] However, the mobility is low, like in the LnOCuCh materials, with a reported value of 0.74 $cm^2\ V^{-1}\ s^{-1}$.[79] $Sr_3Sc_2O_5Cu_2S_2$[11] has a band gap of 3.1 eV[72] (Figure 3) and, in contrast to the

(69) Khabbour, H.; Cario, L.; Boucher, F. *J. Mater. Chem.* **2005**, *15*, 3525.
(70) Ueda, K.; Inoue, S.; Hirose, S.; Kawazoe, H.; Hosono, H. *Appl. Phys. Lett.* **2000**, *77*, 2701.
(71) Sato, H.; Negishi, H.; Wada, A.; Ino, A.; Negishi, S.; Hirai, C.; Namatame, H.; Taniguchi, M.; Takase, K.; Takahashi, Y.; Shimizu, T.; Takano, Y.; Sekizawa, K. *Phys. Rev. B* **2003**, *68*, 035112.
(72) Liu, M.-L.; Wu, L.-B.; Huang, F.-Q.; Chen, L.-D.; Chen, I.-W. *J. Appl. Phys.* **2007**, *102*, 116108.
(73) Yanagi, H.; Tate, J.; Park, S.; Park, C.-H.; Keszler, D. A. *Appl. Phys. Lett.* **2003**, *82*, 2814.
(74) Park, C.-H.; Kykyneshi, R.; Yokochi, A.; Tate, J.; Keszler, D. A. *J. Solid State Chem.* **2007**, *180*, 1672.
(75) Wilmer, D.; Jorgensen, J. D.; Wuensch, B. J. *Solid State Ionics* **2000**, *136−137*, 961.
(76) Ijjaali, I.; Mitchell, K.; Haynes, C. L.; McFarland, A. D.; Van Duyne, R. P.; Ibers, J. A. *J. Solid State Chem.* **2003**, *176*, 170.
(77) Hiramatsu, H.; Ueda, K.; Kamiya, T.; Ohta, H.; Hirano, M.; Hosono, H. *J. Phys. Chem. B* **2004**, *108*, 17344.
(78) Hiramatsu, H.; Ueda, K.; Kamiya, T.; Ohta, H.; Hirano, M.; Hosono, H. *J. Mater. Chem.* **2004**, *14*, 2946.
(79) Ueda, K.; Hirose, S.; Kawazoe, H.; Hosono, H. *Chem. Mater.* **2001**, *13*, 1880.

other materials, a recent report suggests that this compound has the highest mobility of any p-type transparent conducting material with a value of 150 $cm^2\ V^{-1}\ s^{-1}$.[72]

2.1.4. Crystal Chemistry of the Series $A_2ZnO_2M'_2Ch_2$ (A = Sr, Ba; M′ = Cu, Ag; Ch = S, Se). We have been exploring the trends in the structures and properties of the series of wide-band-gap semiconductors $A_2ZnO_2M'_2Ch_2$, where A is Sr or Ba, M′ is Cu or Ag, and Ch is S or Se. The structure is very tolerant of substitutions on these three sites, except that, for the case of A = Ba, M′ = Cu, and Ch = S, the combination of the large alkaline earth and the small chalcogenide renders the structure less stable than a mixture of BaZnOS,[80] $BaSO_4$, $BaCu_2S_2$, Cu, and BaS, and phase separation results. The flexibility in all of these layered structures arises partly from the flexibility of the chalcogenide layer. A much less flexible part of the structure is the MO_2 layer (M = Mn, Co, Ni, Cu, Zn in the known compounds with this structure). The M−O bond length is equal to half of the basal lattice parameter of the tetragonal cell, and incorporation of a larger A^{2+} cation inevitably increases the length of this bond. Incorporation of a larger A^{2+} cation also increases the M−Ch distance, so the M^{2+} ion (Zn^{2+} in the series described here) becomes underbonded as the size of the A^{2+} cation increases. In the most extreme cases that we have explored,[81] $Ba_2ZnO_2Cu_2Se_2$ and $Ba_2ZnO_2Ag_2Se_2$, the structure is retained, but if square-planar coordination of Zn by O is assumed, the four Zn−O distances would exceed 2.1 Å, which is significantly larger than is expected for four-coordinate Zn^{2+} ions by oxide. For comparison, the mean bond length in Ba_2ZnO_3 is 2.00 Å[82] and that in $BaZnO_2$ is 1.98 Å,[83] for both tetrahedral Zn^{2+} ions in the presence of a large electropositive cation. A combination of Zn K-edge EXAFS, powder neutron diffraction, electron diffraction, and single-crystal X-ray diffraction measurements clearly shows that the symmetry of $Ba_2ZnO_2Ag_2Se_2$[81] is reduced from tetragonal *I*4/*mmm* to orthorhombic *Cmca*, and the ideal structure is distorted such that the infinite ZnO_2 square plane fragments into discrete $[ZnO_2]^{2-}$ units arranged in alternating orientations, as shown in Figure 4. The linear coordination environment often found for d^{10} ions such as Hg^{2+} is favored by mixing between the Hg 6s and an O 2p/Hg $5d_{z^2}$-derived state of the same symmetry, and this is promoted by the stabilization of Hg 6s through relativistic effects and because of the lanthanide contraction. Although isoelectronic with Hg^{2+}, the higher energy of the Zn 4s levels means that the driving force for linear coordination is much less strong than that in Hg^{2+} and normally zinc manages to obtain tetrahedral coordination by oxide. Indeed, we have been unable to find other examples of compounds containing discrete $[ZnO_2]^{2-}$ units, although isoelectronic $[ZnN_2]^{4-}$ linear anionic units

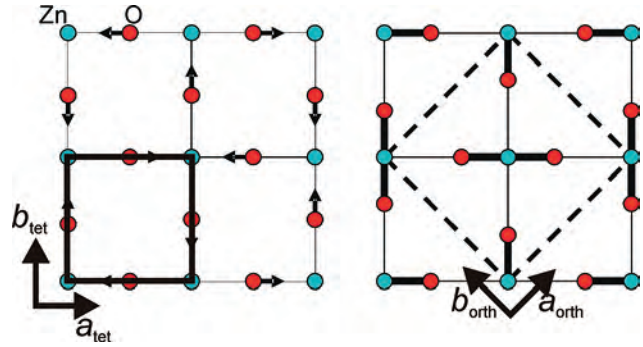

Figure 4. Schematic diagram of the fragmentation of the ZnO_2 plane in $Ba_2ZnO_2Ag_2Se_2$,[81] leading to discrete $[ZnO_2]^{2-}$ anionic units. The left-hand diagram shows the ideal tetragonal cell (bold solid line) and the ordered displacement of oxide ions, which leads to the orthorhombic structure depicted at right (cell indicated by the dotted line). The displacements of the oxide ions are exaggerated.

are found in A_2ZnN_2 (A = Sr, Ba)[84] and Ba_3ZnN_2O.[85] Thus, while the adoption of linear coordination for Zn^{2+} in $Ba_2ZnO_2Ag_2Se_2$ is consistent with that of other d^{10} ions that commonly adopt linear coordination, it seems to require the rather unusual circumstances of a ZnO_2 square plane placed under tension to be realized in practice.

2.2. Interplay of the Composition, Structure, and Magnetic and Electronic Properties in Layered Oxychalcogenides and Oxypnictides. 2.2.1. $CeOCu_{1-\delta}S$. CeOCuS is isostructural with LaOCuS considered above, but cerium is not generally confined to the 3+ oxidation state in compounds containing anions of very electronegative elements such as oxygen. Several reports exist on this compound and appear to conflict with one another. The original report by Charkin et al.[56] showed that the unit cell volume and lattice parameters are contracted relative to the analogues with the neighboring lanthanides but also showed that the compound could be made copper-deficient. Ueda and co-workers[86] reported that the stoichiometric material CeOCuS has a contracted cell volume relative to the expectations of the lanthanide contraction and an effective magnetic moment greatly reduced from the value expected for the $4f^1$ configuration, suggesting that the electrons were not wholly localized on Ce^{3+} ions. More recently, Ibers and co-workers[57] reported single-crystal diffraction results for flux-grown crystals that showed a clear copper deficiency of up to 25% and hence formal oxidation of cerium above the 3+ oxidation state. Our systematic study of this compound[87] showed that a pure, almost stoichiometric, olive-green powder with a copper deficiency of around 2% can be made and that it has the expected localized effective moment for a bona fide Ce^{3+} compound. It also has lattice parameters that conform to the trend shown by the other members of the LnOCuS series and that are larger than those in any previously reported samples of this composition. However, upon exposure to moist air or to pure oxygen, which has been passed through water, the lattice

(80) Broadley, S.; Gál, Z. A.; Corà, F.; Smura, C. F.; Clarke, S. J. *Inorg. Chem.* **2005**, *44*, 9092.
(81) Herkelrath, S. J. C.; Saratovsky, I.; Hadermann, J.; Clarke, S. J. *J. Am. Chem. Soc.* **2008**, submitted for publication.
(82) Scheikowski, M.; Müller-Buschbaum, H. *Z. Anorg. Allg. Chem.* **1992**, *612*, 17.
(83) von Schnering, H. G.; Hoppe, R.; Zemann, J. *Z. Anorg. Allg. Chem.* **1960**, *305*, 241.
(84) Yamane, H.; DiSalvo, F. J. *J. Solid State Chem.* **1995**, *119*, 375.
(85) Yamane, H.; DiSalvo, F. J. *J. Alloys Compd.* **1996**, *234*, 203.
(86) Ueda, K.; Takafuji, K.; Hosono, H. *J. Solid State Chem.* **2003**, *170*, 182.
(87) Pitcher, M. J.; Smura, C. F.; Clarke, S. J. *Chem. Commun.* **2008**, submitted for publication.

parameters shrink and the localized moment decreases, although there is no obvious decomposition of the sample, and no noticeable new Bragg peaks appear in either the X-ray or powder neutron diffractograms. However, close scrutiny using powder neutron diffraction measurements to 0.3 Å in *d* spacing revealed a slight loss of crystallinity (peak broadening), and refinement of the copper site occupancy factor showed that a 15% copper deficiency had developed after 48 h of exposure to a flow of moist oxygen.[87] Extremely broad peaks in the profile of the neutron diffractogram were consistent with the formation of poorly crystalline CuO. Treatment with 5% H_2 restored the lattice parameters, and evidently copper (from the CuO) may be reinjected into the structure, reducing Ce^{4+} to Ce^{3+}. The lattice parameters of the copper-deficient sample obtained by exposure to O_2/H_2O were in excellent agreement with those of a sample made with the composition $CeOCu_{0.85}S$ and with the sample reported by Ueda and co-workers.[86] We conclude that in these compounds copper is highly mobile and may readily be extracted by aerial oxidation. The conclusion from this is that CeOCuS is a well-behaved Ce^{3+} $4f^1$ compound when it is prepared stoichiometrically, but it has a tendency to be oxidized under ambient conditions and the resulting copper deficiency, which is variable and not obvious upon cursory examination, leads to the range of reported lattice parameters for nominally stoichiometric material. The electronic and magnetic properties of the copper-deficient oxidized materials merit further investigation to determine their electronic properties and the extent to which cerium may be oxidized to the 4+ oxidation state in the presence of sulfide.

2.2.2. Electronic Properties of $A_2MO_2Cu_2Ch_2$ Oxychalcogenides. $Sr_2MnO_2Cu_{2m-\delta}S_{m+1}$ ($m = 1-3$; $\delta \sim 0.5$). The homologous series of compounds $Sr_2MnO_2Cu_{2m-\delta}S_{m+1}$ with $m = 1$ (Figure 1), 2, 3 and $\delta \sim 0.5$ (Figure 2) also carry a substantial copper deficiency in the copper sulfide antifluorite-type layers. In the case of the compound originally reported as $Sr_2MnO_2Cu_2S_2$ from powder X-ray diffraction measurements,[9] we showed using single-crystal X-ray and powder neutron diffraction measurements that the correct formulation was $Sr_2MnO_2Cu_{1.5}S_2$ with no indication of a phase width in the composition.[12] The other compounds in the series together with $Sr_4Mn_2O_4Cu_5S_5$,[13] the intergrowth of the $m = 1$ and 2 members, have similar deficiencies per Mn ion, which are similar to the level of deficiency in the most copper-deficient $CeOCu_{1-\delta}S$ samples. Magnetic susceptibility and XANES measurements on the $Sr_2MnO_2Cu_{2m-\delta}S_{m+1}$ ($m = 1-3$; $\delta \sim 0.5$) compounds together with bond-valence analysis showed for all of the members of the series that the Mn ions rather than the states at the top of the valence band are oxidized and have the oxidation state 2.5+.[12] The members of this series are the only examples known in which thick copper sulfide antifluorite-type layers are separated by thin perovskite-type oxide layers, although there are several examples of compounds in which $Cu_{2m}Ch_{m+1}$ layers are separated by large monovalent cations such as K^+,[49] Tl^+.[50,88,89] Structural analysis shows that the

(88) Berger, R.; Eriksson, L. *J. Less Common Met.* **1990**, *161*, 165.

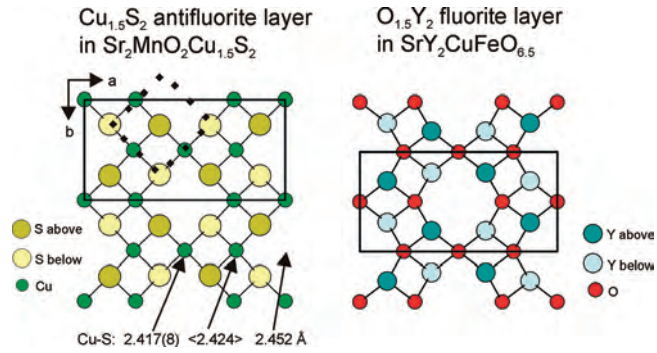

Figure 5. Refined structure of the $Cu_{1.5}S_2$ antifluorite-type layer in $Sr_2MnO_2Cu_{1.5}S_2$ (left) at 100 K showing the ordering of the Cu ions and vacancies. The view is perpendicular to the planes, and the arrangement of sulfide anions above or below the plane of the Cu ions is indicated. The basal dimensions of the enlarged unit cell in *Ibam* [$a = 11.3343(3)$ Å, $b = 5.6700(2)$ Å, $c = 17.0928(2)$ Å] are shown (solid line), as are the basal dimensions of the *I4/mmm* cell (dotted line), which pertains above 240 K when the Cu ions and tetrahedral vacancies are disordered. The mean distances from the Cu ions or the center of the larger, vacant tetrahedral site to the surrounding sulfide ions are indicated. The symmetry of the ordered arrangement is identical with that exhibited by the antitype $O_{1.5}Y_2$ layer in $SrY_2CuFeO_{6.5}$ (right).[91]

Cu ions in the thick sulfide layers are extremely delocalized and probably quite mobile.[12] Low-temperature powder neutron diffraction measurements reveal that in $Sr_2MnO_2Cu_{3.5}S_3$ and $Sr_2MnO_2Cu_{5.5}S_6$ the manganese moments are coupled ferromagnetically within the MnO_2 sheets. This likely arises from a double-exchange-type process mediated by itinerant $d_{x^2-y^2}$ electrons, although further measurements on single-crystal samples are required in order to explore these materials in detail. The planes are coupled antiferromagnetically so the compounds are A-type antiferromagnets. The weak interplanar coupling is readily overcome by an applied magnetic field, and the compounds $Sr_2MnO_2Cu_{3.5}S_3$ and $Sr_2MnO_2Cu_{5.5}S_6$ are metamagnetic and are driven into the ferromagnetic regime by magnetic fields of about 1.3 and 0.06 T, respectively.[12] We report here that the $m = 1$ member of this series $Sr_2MnO_2Cu_{1.5}S_2$ has a different magnetic structure, which appears to be related to the details of the low-temperature crystal structure. The synthesis of this compound is described in ref 12. Powder neutron diffraction measurements (Figures S1 and S2 in the Supporting Information) on $Sr_2MnO_2Cu_{1.5}S_2$ using the diffractometer D2B at the Institut Laue-Langevin, Grenoble, France ($\lambda = 1.59$ Å, $5 \leq 2\theta \leq 160°$) revealed that below 240 K crystallographic ordering of the Cu ions (75% of the tetrahedral sites) and vacancies (25% of the tetrahedral sites) occurs, resulting in a superstructure that is a $2\sqrt{2}a \times \sqrt{2}a \times c$ 4-fold basal expansion of the room temperature structural cell[90] (Figure 5 and Table S1 in the Supporting Information). This shows that the Cu ions must have reasonable mobility in this layer even well below room temperature. The space group of the low-temperature structure is *Ibam* [$a = 11.3343(3)$ Å, $b = 5.6700(2)$ Å, and $c = 17.0928(2)$ Å], and the vacancy ordering in the $Cu_{1.5}S_2$ antifluorite-type layers is similar to that in the fluorite-type $Y_2O_{1.5}$ layers in

(89) Klepp, K. O.; Boller, H.; Voellenkle, H. *Monatsh. Chem.* **1980**, *111*, 727.
(90) Rutt, O. J. D. Phil. Thesis, University of Oxford, Oxford, U.K., 2008.

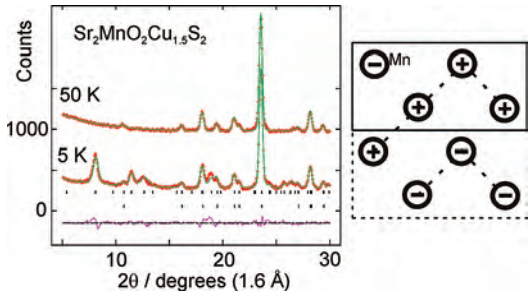

Figure 6. Refinements against powder neutron diffraction data collected on the D2B diffractometer at the ILL, Grenoble, France, on $Sr_2MnO_2Cu_{1.5}S_2$. At 50 K, all of the reflections may be accounted for using the *Ibam* structural model described in Figure 5. At 5 K, below the magnetic ordering transition,[9] the magnetic scattering may be fitted using the "CE"-type model shown at right, in which the moments of 4 μ_B localized on the Mn ions and directed perpendicularly to the MnO_2 planes are arranged in ferromagnetic zigzag stripes that are aligned antiferromagnetically; a single MnO_2 plane within the magnetic unit cell (dotted line) is shown. The data (red points), fit (green line), and difference (shown for 5 K refinement; purple line) are shown; reflection positions for the nuclear (lower) and magnetic (upper) phases are marked. The results of the refinement at 100 K are presented in the Supporting Information.

$SrY_2CuFeO_{6.5}$.[91] Analysis of data collected on D2B at 5 K (Figure 6), below the cusp in the plot of magnetic susceptibility against temperature,[9,12] revealed that the magnetic structure has a cell that is further doubled and is a $2\sqrt{2}a \times 2\sqrt{2}a \times c$ superstructure of the room temperature nuclear cell. The magnetic moments are directed perpendicularly to the MnO_2 planes, like in the members with thicker copper sulfide layers. However, in contrast to $Sr_2MnO_2Cu_{3.5}S_3$ and $Sr_2MnO_2Cu_{5.5}S_4$, which have ferromagnetic MnO_2 planes,[12] the moments within each MnO_2 plane in $Sr_2MnO_2Cu_{1.5}S_2$ are arranged in zigzag ferromagnetic stripes that are aligned antiferromagnetically (Figure 6). This is similar to the CE-type magnetic structure known for the half-doped $Mn^{3+/4+}$ $n = 1$ Ruddlesden−Popper type system $La_{0.5}Sr_{1.5}MnO_4$.[92] In $La_{0.5}Sr_{1.5}MnO_4$, the magnetic structure can be explained by charge ordering of Mn^{4+} and Mn^{3+} ions and orientational ordering of the Jahn−Teller distortion of the Mn^{3+} ions (i.e., orbital ordering). However, in $Sr_2MnO_2Cu_{1.5}S_2$, the extreme anisotropy of the Mn site prevents orbital ordering of the type displayed by $La_{0.5}Sr_{1.5}MnO_4$ and the origin of the CE-type magnetic structure is presumably somewhat different from that in $La_{0.5}Sr_{1.5}MnO_4$ and is currently unclear. The current low-temperature data support the space group assignment *Ibam*, and the structural model contains only one crystallographically unique Mn ion. This argues against long-range charge ordering of distinct Mn^{2+} and Mn^{3+} oxidation states. The selenide analogue of $Sr_2MnO_2Cu_{1.5}S_2$ shows a similar level of copper deficiency but no nuclear superstructure down to 4 K, and it displays the A-type magnetic ordering displayed by $Sr_2MnO_2Cu_{3.5}S_3$ and $Sr_2MnO_2Cu_{5.5}S_6$.[93] The adoption ofthe unusual CE-type magnetic structure in $Sr_2MnO_2Cu_{1.5}S_2$ may therefore be associated with the superstructure adopted by the $Cu_{1.5}S_2$ layer, even though they do not have the same symmetry; further experiments are in progress to determine the link between the crystal and magnetic structures in this compound.

$Sr_2CoO_2Cu_2S_2$. This compound (structure shown in Figure 1) has attracted significant interest in the literature since the first report in 1997[10] because it is an unusual example of high-spin Co^{2+} in a square-planar coordination that is enforced by the layered nature of the crystal structure. Nearest-neighbor Co^{2+} ions couple antiferromagnetically within the CoO_2 planes, but it is also reported that the compound shows unusual spin-glass-like behavior,[94] which may be associated with a slight copper deficiency, which was noted in the original report[10] and which we have confirmed.[93] One report has suggested that at high temperatures the holes arising from copper deficiency are localized on the Co ions, whereas at low temperatures, they become mobile at the top of the valence band.[95] Evidence for this comes from resistivity, thermopower, and the temperature dependence of the dielectric constant,[95] and it is not implausible because the 3d states of a Co^{2+} ion must lie close in energy to the top of the Cu 3d/S 3p-based valence band. However, our recent observation of the subtle air sensitivity of this compound[93] shows that further measurements are required before the true behavior of this compound becomes clear.

$Sr_2NiO_2Cu_2S_2$. Attempts to incorporate reducible late transition metals into the oxide layers of oxychalcogenides are difficult because Ni^{2+} and Cu^{2+} are readily reduced under the conditions that are successfully employed for the synthesis of the Mn and Co analogues (800−1000 °C with low oxygen partial pressure). The existence of $Sr_2NiO_2Cu_2S_2$ and $Sr_2CuO_2Cu_2S_2$ (structure shown in Figure 1) has been reported after synthesis at lower temperatures,[11] but the samples contained large amounts of impurity phases. Decomposition is suppressed at low temperatures, and we have prepared samples of $Sr_2NiO_2Cu_2S_2$ and $Sr_2CuO_2Cu_2S_2$ with purities of 92% and 75%, respectively, by mass by employing a low-melting alkali halide eutectic mixture as a flux.[93] A mixture of composition "$Sr_2NiO_2Cu_2S_2$" was prepared on the 2 g scale in an argon-filled glovebox by grinding together SrS, NiO (Aldrich, 99.99%), and Cu_2O in the molar ratio 2:1:1 under argon. Cu_2O was synthesized by heating Cu (Alfa, 99.999%) and CuO (Aldrich, 99.99%) powders in a 1:1 molar ratio at 1000 °C for 16 h. SrS was made by heating $SrCO_3$ (Alfa, 99.99%) at 800 °C in a flow of CS_2 (Aldrich, 99.5%) vapor carried by flowing argon. This mixture was ground together with a mixture of dry NaI (Alfa, 99.98%) and dry CsI (Aldrich, 99.99%) to give composition 1:0.44:0.56 "$Sr_2NiO_2Cu_2S_2$"/NaI/CsI. The mixture was contained in an alumina crucible sealed inside an evacuated silica tube and heated at 500 °C for three periods of 15 h with intermediate regrinding. The flux was then

(91) Kim, J. S.; Lee, J. Y.; Swinnea, J. S.; Steinfink, H.; Reiff, W. M.; Lightfoot, P.; Pei, S.; Jorgensen, J. D. *J. Solid State Chem.* **1991**, *90*, 331.
(92) Sternlieb, B. J.; Hill, J. P.; Wildgruber, U. C.; Luke, G. M.; Nachumi, B.; Moritomo, Y.; Tokura, Y. *Phys. Rev. Lett.* **1996**, *76*, 2169.
(93) Smura, C. F. D. Phil. Thesis, University of Oxford, Oxford, U.K., 2008.
(94) Okada, S.; Matoba, M.; Fukumoto, S.; Soyano, S.; Kamihara, Y.; Takeuchi, T.; Yoshida, H.; Ohoyama, K.; Yamaguchi, Y. *J. Appl. Phys.* **2002**, *91*, 8861.
(95) Okada, S.; Terasaki, I.; Ooyama, H.; Matoba, M. *J. Appl. Phys.* **2004**, *95*, 6816.

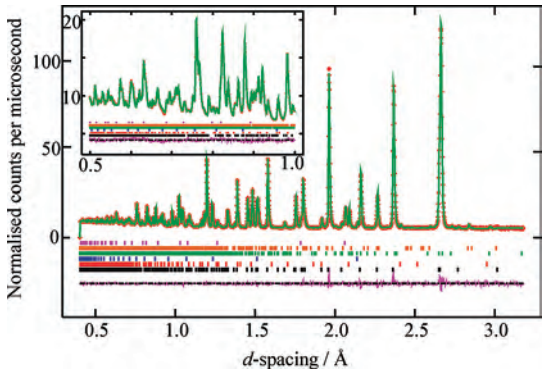

Figure 7. Results of Rietveld refinement of the structure of $Sr_2NiO_2Cu_2S_2$ against POLARIS data at room temperature. The diffractogram collected by the 145° detector bank is shown. The data (red points), fit (green line), and difference plots (lower purple line) are shown. The reflection positions for the phases used in the refinement are indicated (lowest to uppermost): $Sr_2NiO_2Cu_2S_2$ [*I*4/*mmm*; a = 3.92159(2) Å, c = 18.11558(15) Å, V = 278.597(5) Å^3], NiO [1.58(1)% by mass], $SrSO_4$ [1.81(4)%], $SrCO_3$ [0.92(3)%], and $Cu_{0.56}Ni_{0.44}$ [3.38(2)%], respectively. The inset shows the fit in the low d-spacing region. χ^2 = 2.556, R_{wp} = 0.0149, and $R(F^2)$ = 0.0663.

removed by washing with water and acetone. No decomposition of $Sr_2NiO_2Cu_2S_2$ was observed during washing or upon exposure to the atmosphere.

The results of refinement of the crystal structure against powder neutron diffraction data measured at room temperature on the POLARIS diffractometer, ISIS Facility, Oxon, U.K., are presented in Figure 7. The *I*4/*mmm* model used for the other $Sr_2MO_2Cu_2S_2$ compounds was found to be satisfactory. The results of variable-temperature powder neutron diffraction measurements on $Sr_2NiO_2Cu_2S_2$ (Table S2 in the Supporting Information) show several transition regions. Upon cooling from room temperature to 155 K, the c lattice parameter perpendicular to the NiO_2 planes decreases while the basal a lattice parameter increases somewhat (Figure 8). Between 155 and 145 K, the c parameter rises sharply and there is an accompanying increase in the unit cell volume. Below 140 K, the basal lattice parameter a decreases sharply while the c parameter increases steeply, but there is no anomaly in the behavior of the unit cell volume in this region. The *I*4/*mmm* model was adopted successfully over the entire temperature range. The interpretation of the magnetic susceptibility measurements is hampered by the occurrence of some Ni−Cu alloy impurity[96] arising from the decomposition, but the susceptibility of $Sr_2NiO_2Cu_2S_2$ (Figure 8) shows a sharp drop between 180 and 150 K (i.e., above the unit cell volume anomaly), and this is accompanied by a feature in the heat capacity (Figure 8) corresponding to an entropy change of 1 J K^{-1} mol^{-1}. No sharp or broad magnetic scattering is evident in powder neutron diffractograms measured between 5 K and room temperature. Further measurements are required to determine the precise behavior of this compound. The behavior of the Ni−O and Ni−S bond lengths (Figure 9) and lattice parameters (Figure 8) below 140 K shows that the Ni^{2+} coordination environment becomes more square planar upon

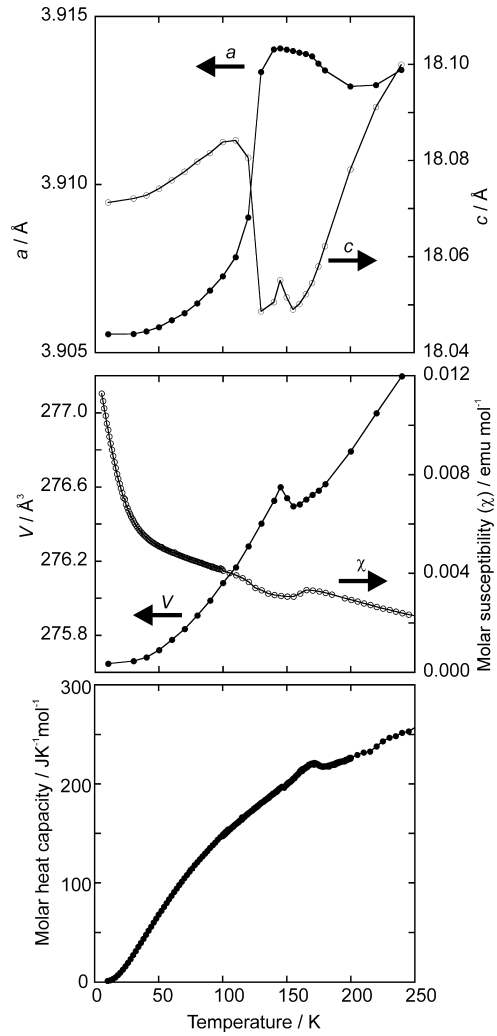

Figure 8. Behavior of the lattice parameters, unit cell volume, molar magnetic susceptibility (1000 Oe applied field), and heat capacity in $Sr_2NiO_2Cu_2S_2$ as functions of temperature. Error bars are smaller than the symbols. The steeply rising portion of the magnetic susceptibility below 50 K arises from the Ni−Cu alloy impurity; the susceptibility anomaly at 170 K coincides with the heat capacity anomaly.

cooling below 130 K and is suggestive of a transition from a high-spin state to a low-spin state upon cooling, but the magnetic signature of this is not evident, possibly because of the presence of the Ni−Cu alloy impurity. The origin of the volume anomaly between 145 and 155 K is also unclear, and further synthetic work is required to attempt to obtain definitive explanations for the observations. This compound, together with the Mn and Co analogues, illustrates the rich behavior of low-dimensional transition-metal compounds, and the oxychalcogenides offer a way to make very rigorously two-dimensional compounds by virtue of the oxide/chalcogenide ordering; this enables unusual coordination environments for the transition metals to be explored.

2.2.3. Superconductivity in Layered Oxypnictides. Recently, superconductivity has been reported in several layered oxide pnictide materials with the ZrSiCuAs structure type (Figure 1). The initial reports in this area are reviewed by Johrendt and Pöttgen.[97] Low-temperature superconductivity

(96) Ryan, F. M.; Pugh, E. W.; Smoluchowski, R. *Phys. Rev.* **1959**, *116*, 1106.

(97) Johrendt, D.; Pöttgen, R. *Angew. Chem.* **2008**, *47*, 4782.

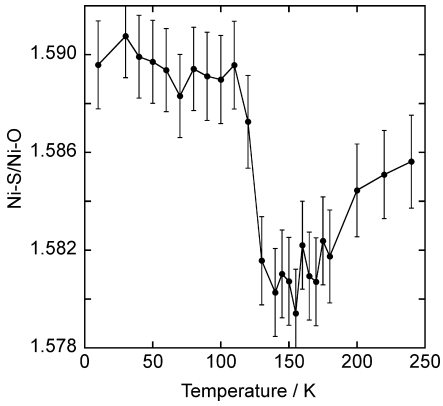

Figure 9. Change in the coordination environment of the Ni ion in $Sr_2NiO_2Cu_2S_2$ as a function of temperature obtained from powder neutron diffraction measurements. The environment becomes significantly more square planar upon cooling below 130 K.

($T_c = 4$ K) was initially reported in apparently stoichiometric LaOFeP, while 6% doping by F on the O site (electron doping) raised T_c to 6 K.[98] Stoichiometric LaONiP was also reported to be a low-temperature superconductor,[99] However, the interest of the community was piqued by the observation by Hosono and co-workers of much higher values of T_c in a series of oxyarsenide analogues. LaOFeAs is an antiferromagnetic insulator with a small ordered moment of about 0.3 μ_B on the Fe atoms.[100] It may be electron-doped into the metallic regime either by the substitution of fluoride for oxide or by the incorporation of oxide deficiency. In both cases, superconductivity occurs below about 26 K in $LaO_{1-x}F_xFeAs$ ($0.07 < x < 0.12$)[101] or $LaO_{1-x}FeAs$ ($x \sim 0.15$).[102] In $LaO_{1-x}F_xFeAs$, the superconducting transition temperature T_c can be raised as high as 43 K by the application of pressure.[103]

Substitution of a smaller lanthanide apparently raises T_c with transition temperatures of 50 K reported in $PrO_{0.85}F_{0.15}FeAs$[104] and $NdO_{0.85}F_{0.15}FeAs$[105] and the largest value of 55 K for this series occurring for oxide-deficient $SmO_{0.85}FeAs$.[102] Although the initial report noted that hole doping via substitution of Ca^{2+} for La^{3+} failed to induce superconductivity, more recent studies of Sr-doped materials suggest that $La_{0.88}Sr_{0.12}OFeAs$ also superconducts below about 25 K.[106]

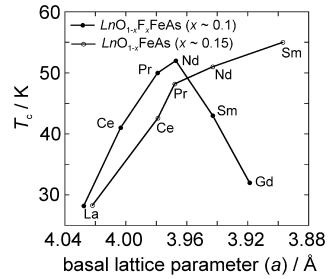

Figure 10. Maximum reported T_c vs basal lattice parameter in $LnO_{1-x}F_xFeAs$ and $LnO_{1-x}FeAs$.

The trend in T_c with the lattice parameter ($=\sqrt{2} \times$ Fe−Fe distance) is shown in Figure 10 for the fluoride-doped and oxide-deficient materials. In addition to the electron count, the bond angles and interatomic separations in the FeAs layer presumably have an important influence on the superconductivity. The observation of both hole- and electron-doped superconductivity offers some similarities with the cuprate-based superconductors. At this time, the investigation of this new class of superconductors is at a very preliminary stage. What is clear is that there exist many ways to modify the electronic properties of these compounds with the ZrSiCuAs ($HfCuSi_2$) structure type. Like in the layered cuprate superconductors, the behavior of the charge-carrying (FePn) layer is influenced by chemical substitution in the "charge-reservoir" (LnO) layer, and most investigations have centered on electron doping via substitution of the oxide anions by fluoride anions or by vacancies. The synthesis of pure samples is difficult, requiring high temperatures, and often high pressures under anaerobic conditions, and in the fluoride-doped materials and those in which substitution has been carried out on the lanthanide site, the presence of binary fluoride and/or other impurity phases makes the precise composition of the superconducting phases very uncertain. Values of T_c above 40 K, upper critical fields that exceed the Bardeen-Cooper-Schrieffer (BCS) limit,[107] and several preliminary theoretical arguments suggest that, like in the cuprates, the superconductivity in these phases is unconventional (i.e., non-BCS) with no obvious limit on T_c. Further experimental and theoretical work on these compounds will attempt to establish the pairing mechanism and answer such questions as whether antiferromagnetic spin fluctuations in the FeAs layers play a role in the superconductivity, whether the paramagnetism of the Ln ions has an effect on T_c, and how similar these new materials are to the superconducting cuprates. In the absence of a clear mechanism for superconductivity, the potential for raising T_c is unclear. Because superconductivity has also been reported in compounds with FeP and NiP antifluorite-type layers and in pure arsenides containing anti-PbO-type FeAs layers,[108] further synthetic work will attempt to establish whether, like in the cuprates, there are several structure types that can support superconductivity in anti-PbO-type or antifluorite-type transition-metal

(98) Kamihara, Y.; Hiramatsu, H.; Hirano, M.; Kawamura, R.; Yanagi, H.; Kamiya, T.; Hosono, H. *J. Am. Chem. Soc.* **2006**, *128*, 10012.
(99) Watanabe, T.; Yanagi, H.; Kamiya, T.; Kamihara, Y.; Hiramatsu, H.; Hirano, M.; Hosono, H. *Inorg. Chem.* **2007**, *46*, 7719.
(100) de la Cruz, C.; Huang, Q.; Lynn, J. W.; Li, J.; Ratcliff, W.; Zarestky, J. L.; Mook, H. A.; Chen, G. F.; Luo, J. L.; Wang, N. L.; Dai, P. *Nature* **2008**, *453*, 899.
(101) Kamihara, Y.; Watanabe, T.; Hirano, M.; Hosono, H. *J. Am. Chem. Soc.* **2008**, *130*, 3296.
(102) Ren, Z.-A.; Che, G. C.; Dong, X.-L.; Yang, J.; Lu, W.; Yi, W.; Shen, X.-L.; Li, Z.-C.; Sun, L.-L.; Zhou, F.; Zhao, Z.-X. *Europhys. Lett.* **2008**, *83*, 17002.
(103) Takahashi, H.; Igawa, K.; Arii, K.; Kamihara, Y.; Hirano, M.; Hosono, H. *Nature* **2008**, *453*, 376.
(104) Ren, Z.-A.; Yang, J.; Lu, W.; Yi, W.; Che, G.-C.; Dong, X.-L.; Sun, L.-L.; Zhao, Z.-X. *Mater. Res. Innovations* **2008**, *12*, 1.
(105) Ren, Z.-A.; Yang, J.; Lu, W.; Yi, W.; Shen, X.-L.; Li, Z.-C.; Che, G. C.; Dong, X.-L.; Sun, L.-L.; Zhou, F.; Zhao, Z.-X. *Europhys. Lett.* **2008**, *82*, 57002.
(106) Wen, H.-H.; Mu, G.; Fang, L.; Yang, H.; Zhu, X. *Europhys. Lett.* **2008**, *82*, 17009.
(107) Hunte, F.; Jaroszynski, J.; Gurevich, A.; Larbalestier, D. C.; Jin, R.; Sefat, A. S.; McGuire, M. A.; Sales, B. C.; Christen, D. K.; Mandrus, D. *Nature* **2008**, *453*, 903.
(108) Rotter, M.; Tegel, M.; Johrendt, D. *Phys. Rev. Lett.* **2008**, in press.

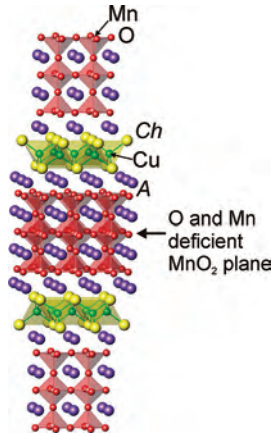

Figure 11. Crystal structure of $A_4Mn_2O_{7.5}Cu_2Ch_2$ (A = Sr, Ba; Ch = S, Se)[17,19] consisting of Cu_2Ch_2 antifluorite layers separating perovskite-type alkaline-earth manganite layers. Mn and oxide deficiencies occur in the central plane of the oxide block, and the mean Mn oxidation state is 3+.

pnictide layers. Several oxyphosphides, oxyarsenides, and oxyantimonides with MnPn and ZnPn antifluorite-type layers exist including $Sr_2MnO_2Mn_2Sb_2$,[6] the first representative of the crystal structure (Figure 1) adopted by many of the oxychalcogenides discussed above. The synthesis, structures, and magnetic properties of several of these compounds have been investigated by Kauzlarich and co-workers.[7,8] It may be that related systems in which perovskite-type oxide blocks separate middle-to-late transition-metal pnictide layers may prove to be superconducting if the electron count and lattice parameters can be tuned appropriately.

2.3. Chemical Properties. 2.3.1. $Sr_4Mn_3O_{7.5}Cu_2Ch_2$ Series. The manganite layer in $Sr_4Mn_3O_{7.5}Cu_2S_2$ and the selenide analogue resembles a fragment of the perovskite structure (Figures 2 and 11). As pointed out by Zhu and Hor in their original report on compounds with this structure type,[17] there is a significant oxide deficiency (about one-quarter) in the central portion of the manganite layer. Furthermore, our single-crystal X-ray and powder neutron diffraction measurements showed that in the case of the oxysulfides, but not the oxyselenides, there is a small manganese deficiency in the central layer.[19] The disorder inherent in the central layer results in glassy behavior of the manganese moments in the central layer, while the Mn ions in the outer layers of the oxide slab order antiferromagnetically. This is analogous to the behavior in some $n = 3$ Ruddlesden−Popper oxide materials[109] and in the analogous oxychloride $Sr_4Mn_3O_{7.56}Cl_2$.[110] Subsequent investigations revealed that these compounds, synthesized using standard solid-state techniques, albeit with the samples sealed in silica tubes, are susceptible to both low-temperature oxidation and reduction. Reduction was carried out by reacting the oxychalcogenides with sodium hydride in sealed glass ampules at about 200 °C, as originally described in the synthesis of $LaNiO_2$.[52] This introduced further vacancies on the oxide sublattice and chemical disorder due to the reduction of manganese and was found to completely destroy the long-range-ordered magnetic structure. Conversely, oxidation by insertion of fluorine from XeF_2[111] was also possible and resulted in filling of the vacant anion sites and an increase in the the size of the long-range-ordered moment.[19] These substantial changes in composition achieved under mild conditions suggest possible application as heterogeneous redox catalysts, and this is under investigation.

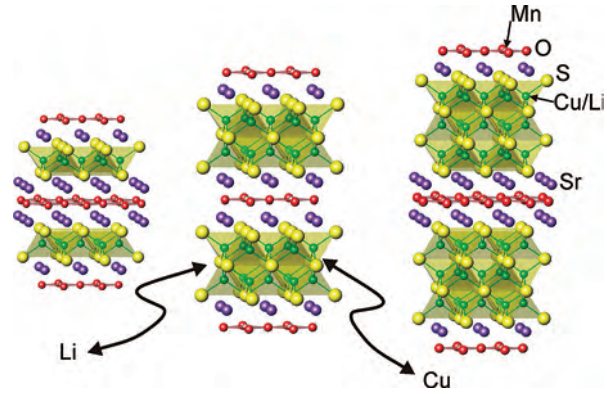

Figure 12. Schematic diagram indicating the reversible insertion/extrusion of lithium into the series $Sr_2MnO_2Cu_{2m-0.5}S_{m+1}$ [$m = 1$ (left), 2 (middle), and 3 (right)].[14,15]

2.3.2. $Sr_2MnO_2Cu_{2m-\delta}S_{m+1}$ as Potential Battery Electrode Materials. The crystal structures of the members of this series with thicker copper sulfide layers ($m = 2, 3$)[12] (Figures 2 and 12) show that the Cu ion scattering density is extremely delocalized and suggests that the Cu ions may be highly mobile in these compounds, as are the Ag^+ ions in LaOAgS.[75] The low-temperature cation/vacancy-ordered superstructure of $Sr_2MnO_2Cu_{1.5}S_2$ reported here also demonstrates that there must be reasonable Cu ion mobility in these copper sulfide layers at ambient temperatures. To underline the mobility of the Cu ions in the sulfide layers of these oxysulfides, the reaction of the compounds $Sr_2MnO_2Cu_{2m-\delta}S_{m+1}$ with *n*-BuLi in hexane at room temperature results in complete replacement of the Cu^+ ions in the sulfide layers by Li^+ ions and extrusion of elemental copper onto the surface of the particles, as indicated schematically in Figure 12.[14] The process is quasi-reversible in moist air: Li ions are extracted as lithium hydroxide and copper reinserts into the structure.[14]

Collaboration with Grey and co-workers[15] showed that the lithium insertion/copper extrusion process[112] may be carried out reversibly in an electrochemical cell and also showed using Li NMR spectroscopy that the Li ions in the sulfide layers are highly mobile.[15] The development of battery electrode materials using the principle of lithium insertion and extrusion of a transition metal has been pursued in several oxide and sulfide systems.[112] In the case of Cu_2S[15], the reversibility over several cycles is poor, while in the oxysulfides, which effectively represent slabs of the Cu_2S structure separated by the oxide layers, cyclability is much better, perhaps because the rigid oxide layers prevent structural collapse.

(109) Battle, P. D.; Green, M. A.; Lago, J.; Millburn, J. E.; Rosseinsky, M. J.; Vente, J. F. *Chem. Mater.* **1998**, *10*, 658.
(110) Knee, C. S.; Zhukov, A. A.; Weller, M. T. *Chem. Mater.* **2002**, *14*, 4249.
(111) Ardashnikova, E. I.; Lubarsky, S. V.; Denisenko, D. I.; Shpanchenko, R. V.; Antipov, E. V.; Van Tendeloo, G. *Physica C* **1995**, *253*, 259.
(112) Morcrette, M.; Rozier, P.; Dupont, L.; Mugnier, E.; Sannier, L.; Galy, J.; Tarascon, J.-M. *Nat. Mater.* **2003**, *2*, 755.

3. Conclusions

The area of mixed-anion chemistry offers materials complementary to those of other classes, notably the oxides, which have been studied far more extensively. In this Forum Article, we have briefly surveyed the area of layered oxychalcogenide and oxypnictide chemistry and have shown how the compounds show promise in areas as diverse as transparent conductors and battery materials as well as demonstrated some unusual structural, magnetic, and chemical properties. Recent discoveries have demonstrated the importance of the investigation of new and unusual classes of material. In a 2005 survey of "contemporary superconductors",[113] Cava concluded that "just when it looks like all the possibilities have been tried, someone will find a new superconductor that will change the direction of the field." The discovery of the high-temperature oxypnictide superconductors has borne this out, and the solid-state chemistry and physics community is currently working to understand the physics of this class of material. We can propose that these layered mixed-anion compounds may eventually be technologically important and can conclude with more certainty that they are important in understanding the ways in which electrons behave in solids.

Acknowledgment. We thank the U.K. Engineering and Physical Sciences Research Council for funding under Grants GR/N17853 and EP/E025447 and for the award of studentships to O.J.R., C.F.S., S.J.C.H., P.A., and M.J.P. We thank Dr. R. I. Smith, Dr. K. Knight, Dr. R. M. Ibberson, Dr. M. Telling (ISIS Facility), and Dr. A. Hewat and Dr. E. Suard (ILL) for assistance with the PND measurements and Prof. A. T. Boothroyd, Dr. D. Prabhakaran, and P. Baker (Department of Physics, University of Oxford, Oxford, U.K.) for the heat capacity measurement. We acknowledge extremely fruitful collaborations with the groups of Prof. C. P. Grey (SUNY Stony Brook, Stony Brook, NY) in the area of battery materials and solid-state NMR measurements and Prof. J. Hadermann (EMAT, University of Antwerp, Antwerp, Belgium) for collaboration in the area of electron microscopy and diffraction.

Supporting Information Available: Refinement results, atomic coordinates, and thermal and structural parameters. This material is available free of charge via the Internet at http://pubs.acs.org.

IC8009964

(113) Cava, R. J. *Chem. Commun.* **2005**, 5373.